# Mystery Solved: Five Surprises Discovered With Megahertz Sampling and Traveling-Wave Data Analysis

Edmund O. Schweitzer, III, Veselin Skendzic, Armando Guzmán,
Mangapathirao V. Mynam, and Jean León Eternod
*Schweitzer Engineering Laboratories, Inc.*

Yanfeng Gong
*American Electric Power*

Presented at the
FISE IEEE/CIGRE Conference
Medellín, Colombia
December 4–6, 2019

Previously presented under the current title at
RVP-AI 2019, July 2019, and
72nd Annual Conference for Protective Relay Engineers, March 2019

Previously presented under the original title at the
XIV Simposio Iberoamericano Sobre Proteccion de Sistemas
Electricos de Potencia, February 2019

Originally presented at the
45th Annual Western Protective Relay Conference, October 2018, under the title
"Five Surprises Discovered With Megahertz Sampling and Traveling-Wave Data Analysis"

# Mystery Solved: Five Surprises Discovered With Megahertz Sampling and Traveling-Wave Data Analysis

Edmund O. Schweitzer, III, Veselin Skendzic, Armando Guzmán, Mangapathirao V. Mynam, and Jean León Eternod, *Schweitzer Engineering Laboratories, Inc.*
Yanfeng Gong, *American Electric Power*

***Abstract*—High-frequency traveling-wave technology is entering the power system application mainstream, bringing with it an unprecedented level of highly accurate signal detail. High-frequency traveling-wave transients have proven their practical value for ultra-high-speed protection and accurate fault locating.**

**This paper presents the rest of the story, documenting and explaining some of the more surprising, lesser-known, and strange-looking waveforms captured while monitoring high-voltage transmission lines. The paper also explains the limitations and distortion introduced by conventional secondary wiring systems, helping the practicing engineer interpret detailed event data captured by the latest generation of protective relays and digital fault recording systems.**

**Special emphasis is given to monitoring primary apparatus health and identifying high-voltage system sources generating the traveling-wave transients. Transient modeling, Bewley diagrams, and spectral analysis methods are also used to analyze the data.**

## I. Introduction

Traveling-wave-based protective relays with high-resolution megahertz sampling capability have recently opened a new window into the high-voltage transmission system operation. Continuously available (24/7), these relays keep constant watch over the power system, recording large numbers of transient events that were previously unknown. Over a two-year recording campaign, we collected over twenty thousand event records. Events span almost all application and voltage levels, from monitoring a 765 kV transmission network, down to analyzing a 13.8 kV shunt reactor switching transient.

This paper presents five of those events along with the system data and multiple analysis details. Of special interest are the events that did not lead to breaker trips, because they could be used proactively for predictive maintenance. Repetitive events from the same geographic location may be indicative of failing electrical equipment, a contaminated insulator, or a failing instrument transformer. Events from the same geographic location may also indicate severe lightning activity in a specific location and warrant improving shielding for power lines in the area. Utilities are interested to learn if they can use such precursors to justify implementing preventive measures.

## II. Breaker Health Monitoring

We begin by looking at breaker health monitoring: a well-known and commonly expected benefit of high-quality data acquisition. Megahertz sampling provides an exceptionally detailed record of every breaker operation, including pole sequencing, pre-insertion resistor health, reignitions, and restrikes.

Relays equipped with megahertz data acquisition capability recorded breaker activity when energizing a 230 kV, 28.4 km line. Fig. 1 shows the currents and voltages captured by the relay at the local terminal during line energization.

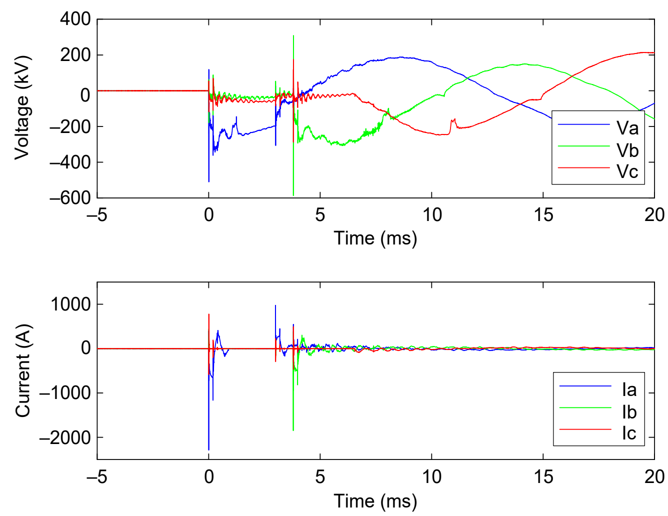


Fig. 1. Currents and voltages recorded while energizing the 230 kV line at the local terminal.

From Fig. 1, we can see that the A-phase closed first, at T = 0. The B-phase closed at T = 3.8 ms, and the C-phase closed at T = 6.5 ms. The A-phase unexpectedly opened at T = 0.9 ms and then closed again at T = 3 ms.

Fig. 1 contains a legend where A-phase waveforms are blue, B-phase waveforms are green, and C-phase waveforms are red. This color scheme is used consistently throughout the paper.

The traveling-wave (TW) detail in Fig. 2 shows that the relay recorded the initial transient from the breaker closing and the subsequent reflection from the open terminal that are visible around 0.2 ms and 0.4 ms.

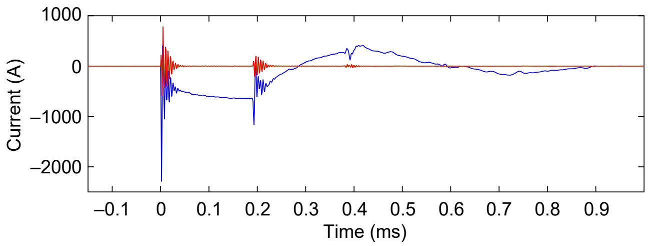


Fig. 2. A-phase closing event initiated TW transients.

Fig. 3 shows the currents and voltages that were captured when the same line was energized from the remote terminal. Based on the currents captured in this event, we can see that the remote breaker did not exhibit the same behavior as the local breaker.

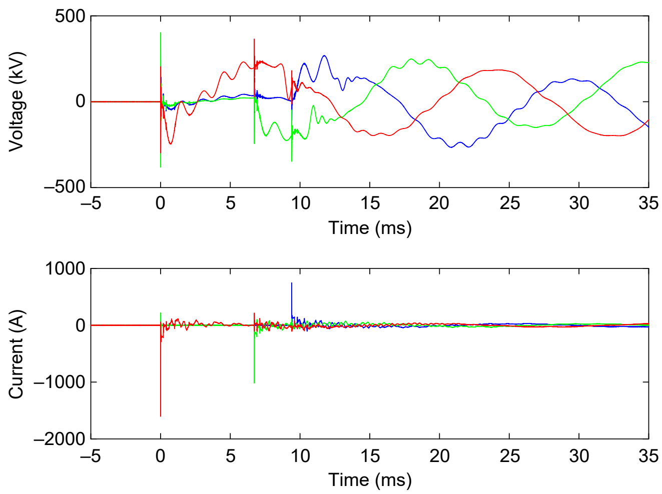


Fig. 3. Currents and voltages recorded while energizing the line at the remote terminal.

The remote breaker closing operation is clean with no unexpected transients. However, the breaker pole discordance is relatively high, with the time difference between the first and last pole closures reaching 10 ms. Because the typical pole discordance times are on the order of 2 to 3 ms, this 10 ms difference raises questions about possible mechanism misalignment.

When analyzing breaker operation, it is important to consider the event type and the breaker technology involved. Switching events with very low current, such as energizing of a very short (28.4 km) overhead line with modest charging current (18 A), may exhibit temporary current interruption during closing operation (Fig. 1). Such behavior depends on the interrupting medium, internal breaker construction, and the number of moving contacts in the given design. In some cases, this type of breaker behavior may warrant preventive breaker inspection.

## III. Fault Current Interruption

Continuing on the breaker operation topic, it is interesting to take a look at the high-resolution record documenting the B-phase-to-ground fault on a 161 kV line in northern Idaho. The line is operated by the Bonneville Power Administration (BPA) and is 117.1 km (72.7 mi) long. At the time of the event, operators reported storm activity in the area. Fig. 4 shows the waveform collected during the fault. It is easy to identify the initial fault transient as well as the current interruption clearing the fault. Two of the phases were cleared in slightly over 2.5 cycles, with the B-phase event lasting over 3 cycles. One thing that immediately stands out is a set of high-frequency transients present in the last half cycle of the fault (B-phase).

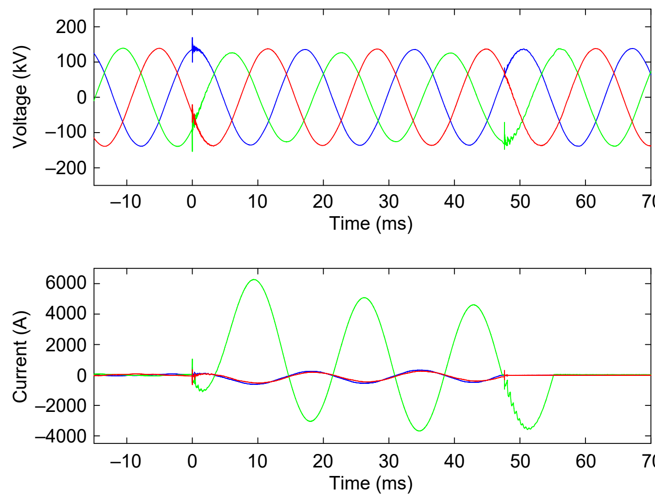


Fig. 4. B-phase-to-ground fault recorded on a 161 kV line in northern Idaho.

Magnifying the initial fault transient in Fig. 4 gives us Fig. 5. Using this high-resolution waveform and a Bewley diagram [1][2], we can isolate the TWs and identify the fault location as 65.5 km (40.71 mi) from the terminal (see Fig. 6).

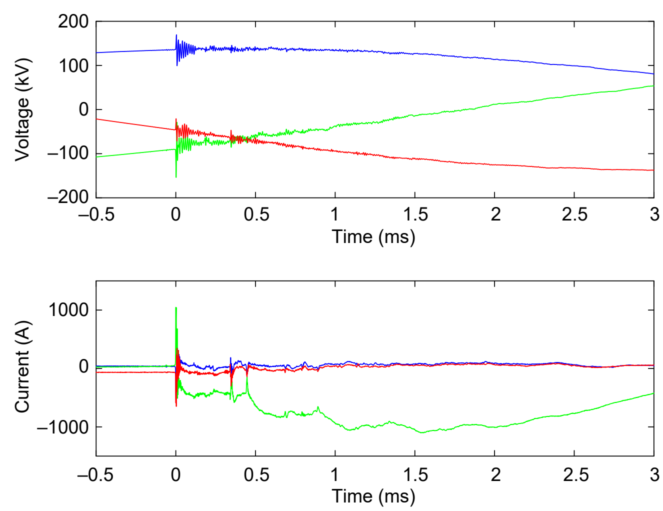


Fig. 5. Detail of Fig. 4 showing the fault initiation instant.

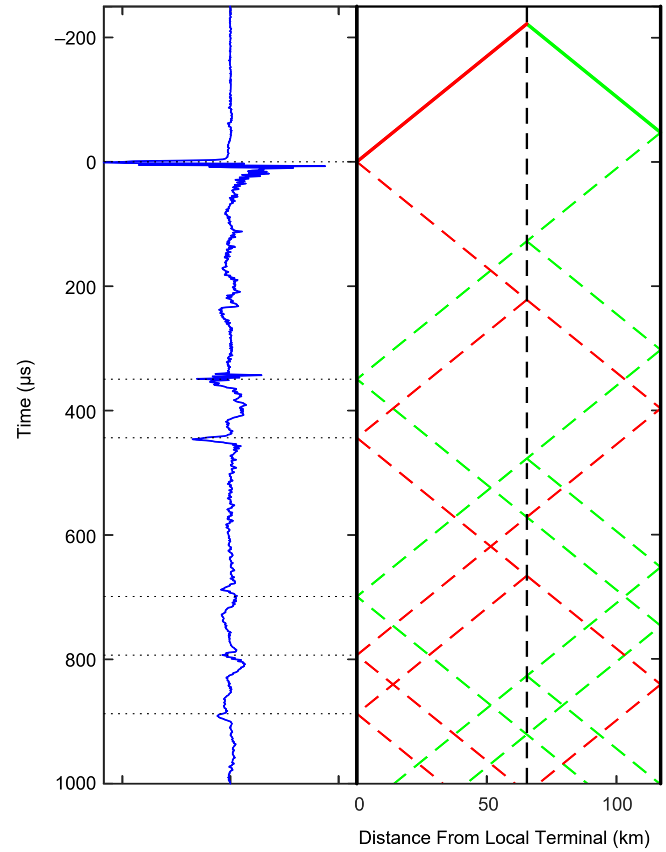


Fig. 6. A Bewley diagram is used to determine the fault location as 65.5 km from the local terminal.

A detailed inspection of the current waveform recorded before the fault, as shown in Fig. 7, allows us to identify the cause of the fault.

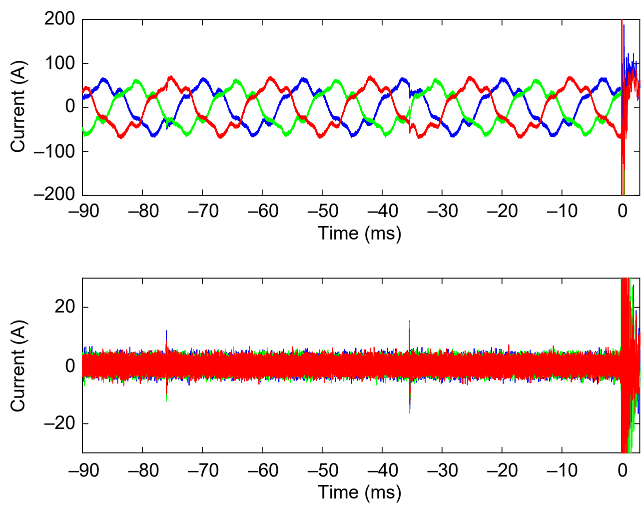


Fig. 7. Magnified section of the current waveform and its high-frequency waveform content recorded within the 90 ms leading up to the fault.

Fig. 7 shows the pre-fault current and its high-frequency content as observed through a differentiator-smoother TW extraction filter [1]. The waveform allows us to identify two precursory events occurring at approximately 76 ms and 35 ms before the fault. Magnifying one of the precursory events, as shown in Fig. 8, we see a common mode current transient with the same shape on all three phases. As explained in detail in the next section, this signature is characteristic of a lightning-induced transient caused by an approaching storm with strikes in the immediate vicinity of the line.

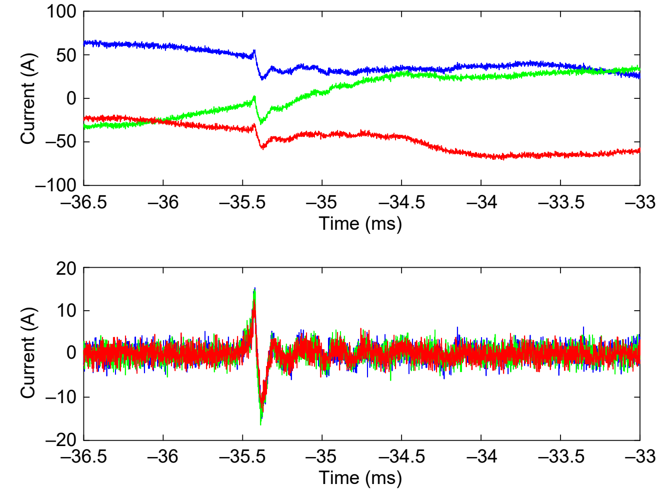


Fig. 8. Current waveform detail with the lightning-induced transient.

Now that we have a high confidence that this fault was caused by a lightning-induced flashover, we can focus our attention on the current interruption and the high-frequency transient visible at the end of the event, as shown in Fig. 9.

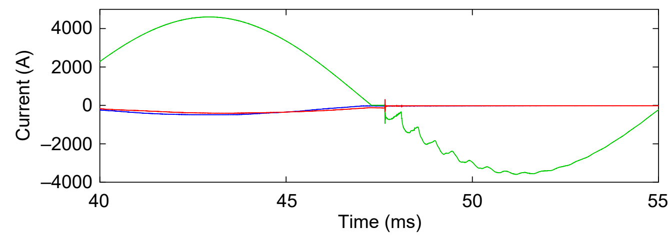


Fig. 9. Current interruption phase.

A-phase and C-phase opened cleanly, with the B-phase reigniting 360 μs after an interruption at the previous current zero. Fig. 10 shows the B-phase reignition detail.

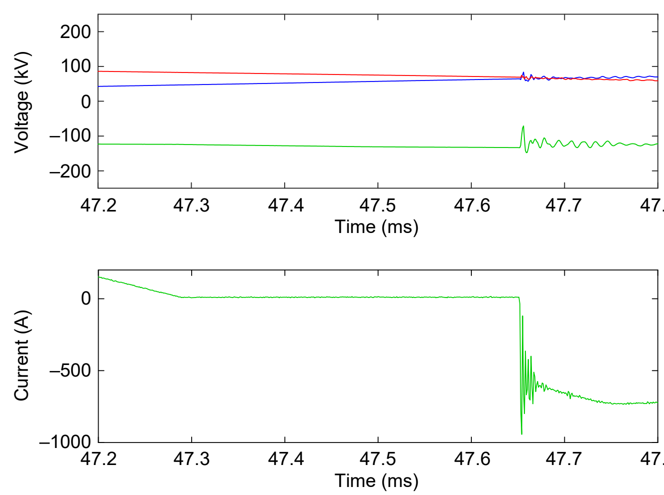


Fig. 10. B-phase current interruption and reignition event.

Fig. 10 shows that the B-phase voltage was very close to its negative peak (–130 kV) at the time of the fault current interruption. As with most of our recordings, it is important to note that the current measurements are typically very faithful and show a broad frequency response, while the voltage measurements show filtering and internal resonances caused by the VT construction. In the case of this particular event, voltage was measured using the bus-connected "magnetic" (traditional) VT shown in Fig. 11a. With the VT connected to the bus side of the breaker, it may be somewhat surprising to see the relatively modest size of the recorded voltage transient. However, we need to keep in mind that the VT filters all waveforms [1] and that the VT location on the bus side made it impossible to see the line voltage leading to the reignition event. Fig. 11b shows the breaker and the capacitively coupled voltage transformer (CCVT) used by other relays on this line.

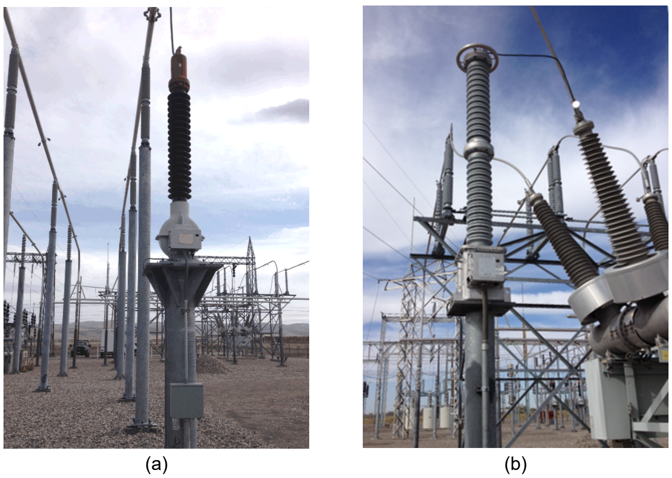


Fig. 11. Bus-connected VT and the line breaker described in the event on the BPA 161 kV line.

Looking at a slightly broader view (Fig. 12), we can see several TW reflections initiated by the reignition event.

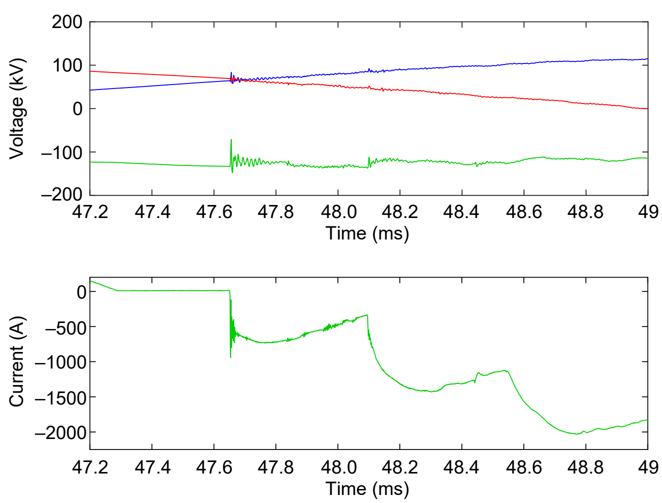


Fig. 12. Reignition event followed by multiple TW reflections.

The Bewley diagram in Fig. 13 provides additional insight for this event. We start by referencing the Fig. 12 reignition transient shown at 47.65 ms as time zero on the Bewley diagram. This transient travels to the previously identified fault location (65.5 km), which is still fully ionized given the short time since current interruption. The transient reflects from the fault, reaching the breaker 445 μs later. The Bewley diagram also shows that the reflection from the far end of the line arrives around 796 μs.

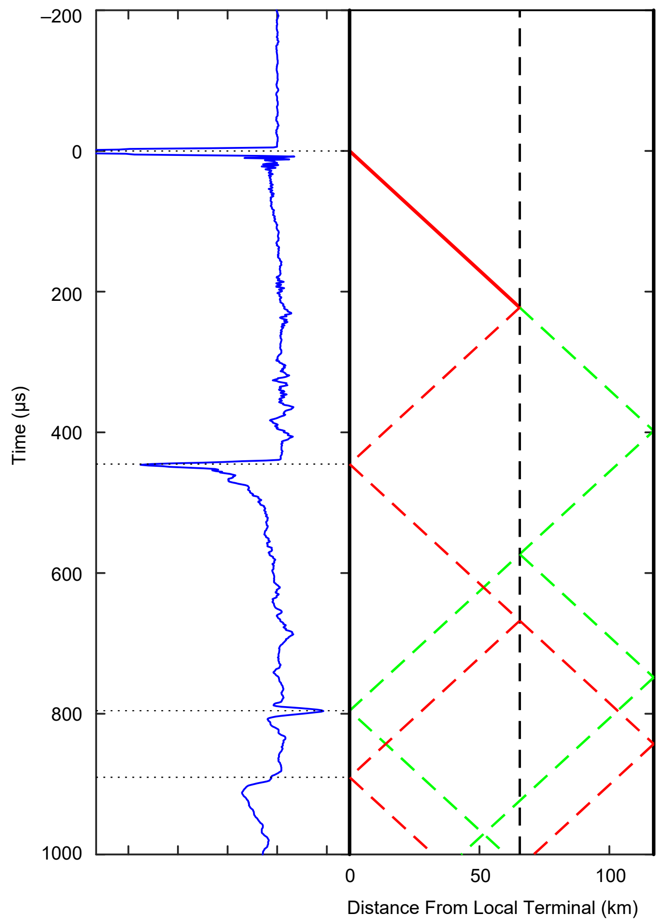


Fig. 13. Reignition event Bewley diagram.

Reignition itself is normal, simply indicating that the B-phase contacts did not have sufficient time to part. Activating the breaker coil several milliseconds earlier may have been sufficient to prevent this reignition event.

## IV. Tracking the Storm

As reported in [3], Comisión Federal de Electricidad (CFE), the electric utility company in Mexico, is operating a long-term high-speed data collection and TW technology evaluation pilot system.

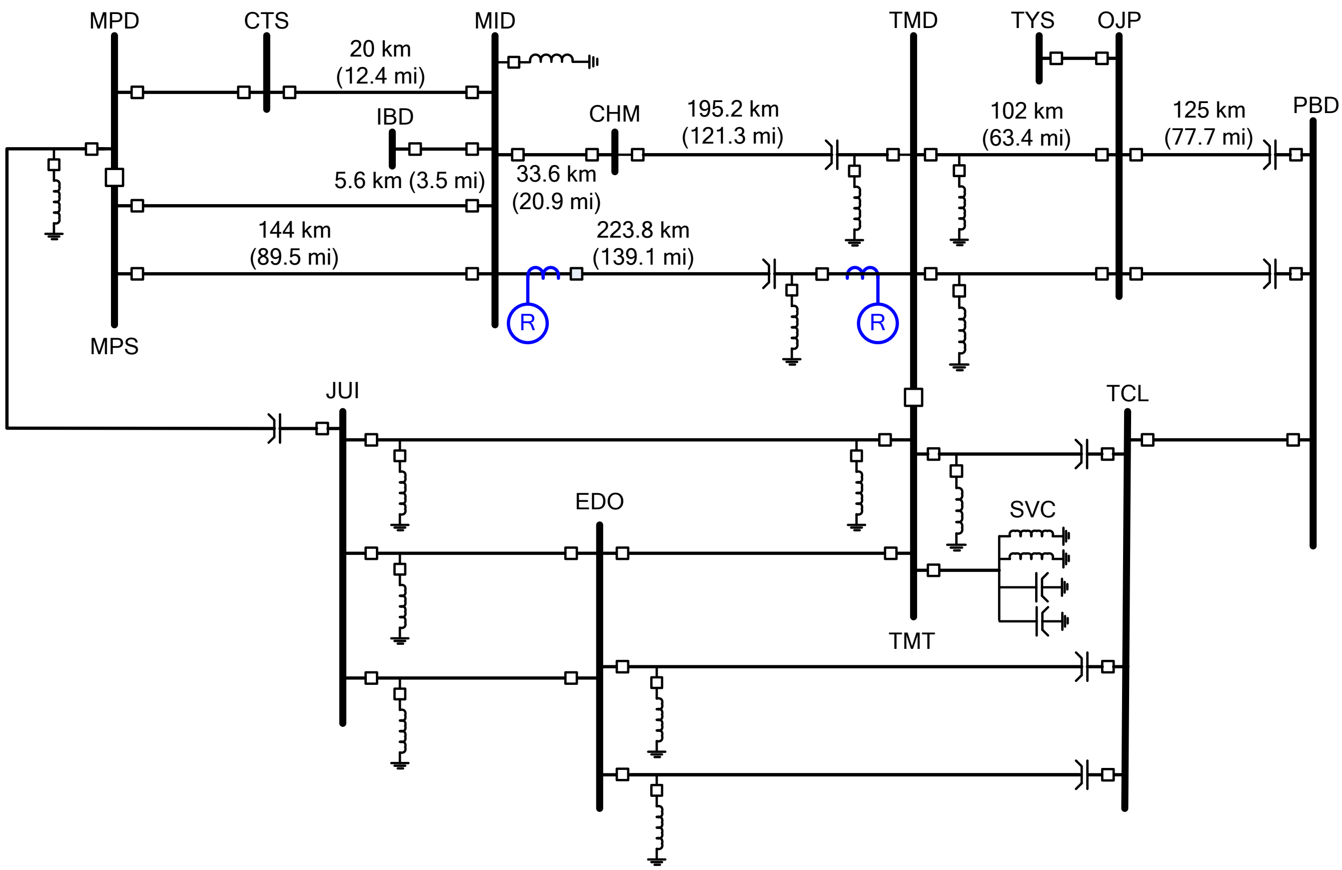


Fig. 14. Event collection is performed on the 400 kV line connecting the MID and TMD substations.

Two relays with megahertz recording capability are installed on the 400 kV series-compensated transmission line that connects substations Minatitlan Dos (MID), located in the state of Veracruz, and Temascal Dos (TMD), located in the state of Oaxaca. The line is 223.8 km long and connects to the rest of the system as shown in Fig. 14.

This transmission line is located in a region with a high incidence of lightning-induced faults, offering an excellent test site for evaluating TW technology potential. The relays are connected to an automatic file retrieval system and are configured with a very sensitive TW detection trigger. To maximize coverage and limit the individual file size, event length is set to 200 ms with pre-fault duration set to 50 ms. The relays are set to trigger independently because of limited communications resources at the sites. They routinely capture faults and power system switching events on neighboring lines as well.

While analyzing the events, we looked for double-ended event records containing TW disturbances that 1) originated inside the line, 2) were not associated with power system faults, and 3) did not result in a relay tripping operation.

Our attention was immediately drawn to a distinct series of TW events occurring on August 1, 2017 and lasting 35 minutes: from 9:50 p.m. to 10:25 p.m. local time. During this interval, the relays collected a total of 32 event records, 20 of which corresponded to TW events simultaneously detected by both relays. A typical waveform captured at the MID substation contains multiple transients, as shown in Fig. 15.

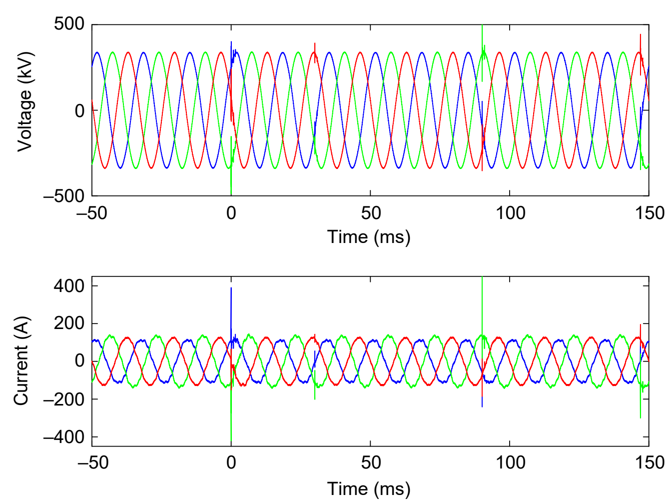


Fig. 15. Typical event record captured at the MID substation.

Fig. 16 shows a magnified portion of the first event, allowing us to note the oscillatory behavior of the voltage waves. The oscillatory behavior in the voltage measurement is caused by the excitation of the power line carrier (PLC) trap, secondary wiring, and the CCVT parasitic capacitance. This behavior is present in virtually all records and is typical for conventional CCVT-based voltage measurements.

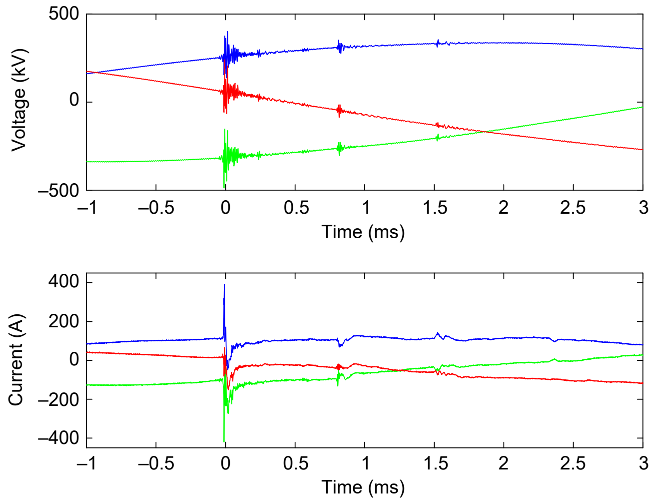


Fig. 16. Detail of Fig. 15 showing the oscillatory behavior of voltage channels and a common mode current transient.

Current measurements provide a more faithful reproduction of the TW, managing to capture a matching exponentially shaped current depression common to all three phases, as shown in Fig. 17. High-frequency oscillations visible at the beginning of the fault (0 ms) are attributed to secondary wiring resonance and can be disregarded in this case.

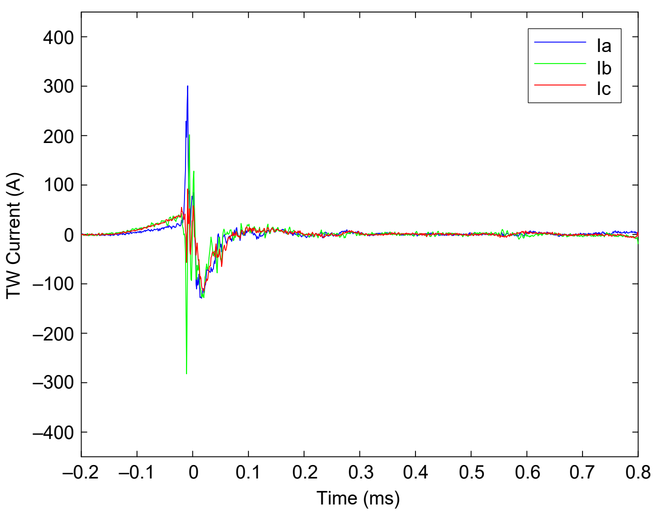


Fig. 17. Common mode current transient after removing the 60 Hz current signal.

A depression is followed by several reflections that are visible in both voltage and current waves. Common mode transients of this nature are not very common because most power system events tend to be phase-specific (caused by the fault or breaker operation on a given phase).

Looking at the same event from the TMD side, we found a very similar wave signature, as illustrated in Fig. 18. Fig. 18 compares the A-phase current waveform recorded at each line end (MID and TMD).

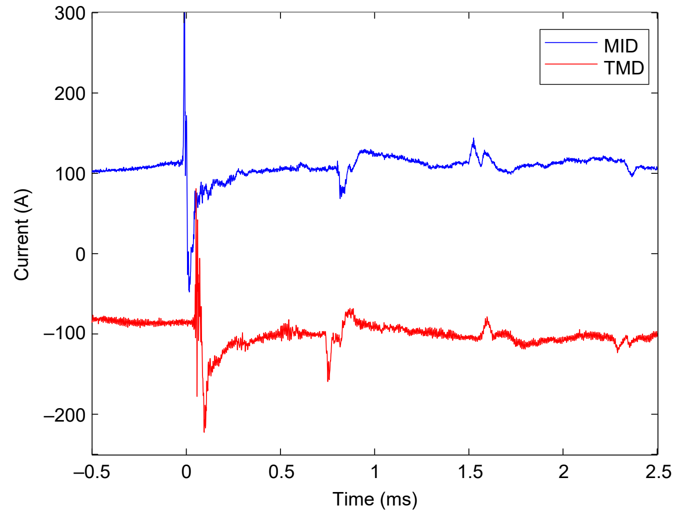


Fig. 18. A-phase current TW transient observed at each line end.

TW arrival times are very close, with the MID wave arriving only 64 µs before the TMD wave, clearly placing this transient between the transmission line terminals. The Bewley diagram for this event, shown in Fig. 19, places the source of this transient at 102.5 km from the MID terminal. It is interesting to note we are not looking at a typical fault event because there are no reflections from the location at which the incident occurred.

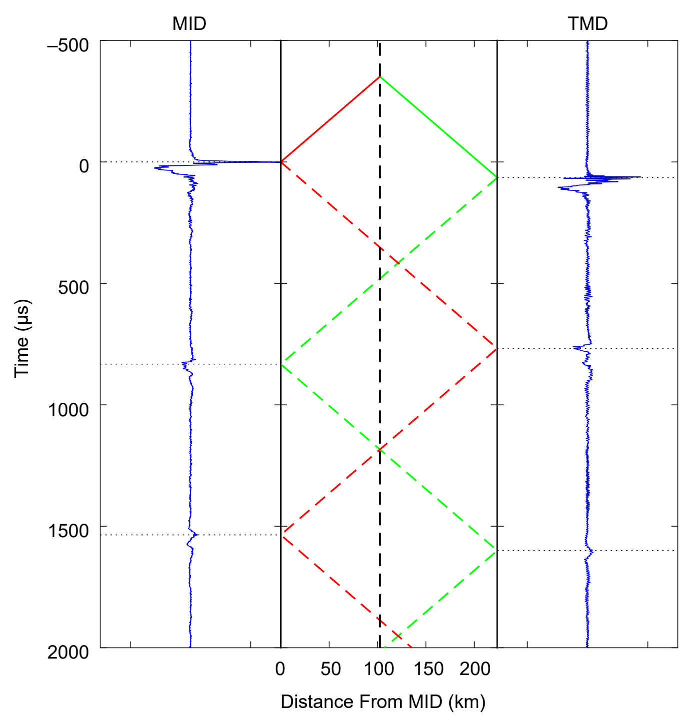


Fig. 19. A Bewley diagram aligned with A-phase current waveforms places the fault at 102.5 km from the MID terminal.

The number of records and the transient nature of this event series motivated us to perform fault-locating analysis for all 32 records. We analyzed single-ended records using a single-ended TW fault-locating algorithm and confirmed results using the 20 double-ended records. Our primary goal was to identify the exact location of the transient source, thus turning this event series into actionable data. However, although the transient event location was somewhat consistent, the exact location appeared to move. Fig. 20 shows how the source location evolved over time.

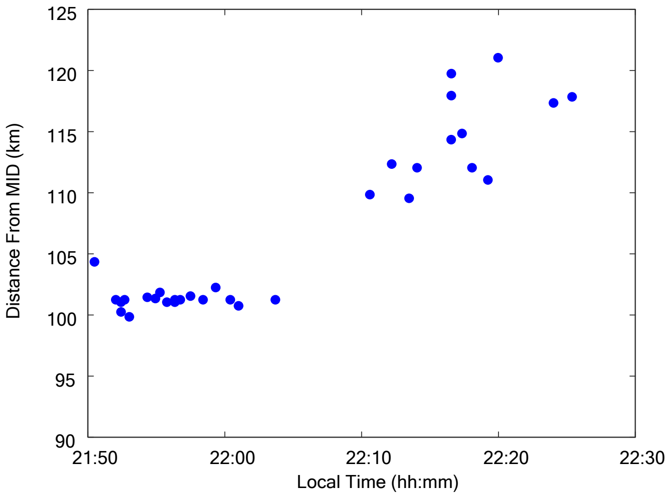


Fig. 20. Transient event location tracks an electrical storm.

Additional analysis determined that the events were not correlated to power system faults. Following is a short summary of our observations:

- The relays recorded 32 events over 35 minutes.
- Most records contain multiple transients, bringing the total number of discrete events to over 60.
- Events are not correlated to a particular power system phase voltage.
- All events originate inside the transmission line.
- Event signatures match among phases and are characterized with a common mode transient.
- All disturbances travel through the transmission line and show multiple reflections.
- Differential current calculations show transient current was injected into the line. The injected current shape loosely matches the standardized 1.2 by 50 µs lightning test waveform.
- The transient injection site moves over time.
- The transmission line traverses a tropical zone known for high lightning activity.

Based on the above observations, we concluded that the events observed on August 1, 2017 were caused by a lightning storm with many nearby strikes to ground or between clouds. Because all the recorded events have matching signatures and modest amplitude, we suspect that none of the strikes were direct hits to the transmission line towers or the ground wires. The lack of power system faults during this period provides additional support for our analysis.

## V. Transmission System Health Monitoring

Better understanding of the substation electromagnetic environment is one of the less expected benefits of the high-frequency TW technology deployment. Over the course of this study, we confirmed that high-voltage (HV) and extra-high-voltage (EHV) substation measurements obtained using conventional instrument transformers, normal secondary wiring, and standard substation construction practices were exceptionally clean and noise free.

However, after installing relays with megahertz recording capabilities at the CFE 400 kV line between the MID and TMD substations, we noticed the presence of intermittent high-energy discharge events. Fig. 21 shows the high-energy discharge waveforms recorded on July 1, 2017 at the MID substation.

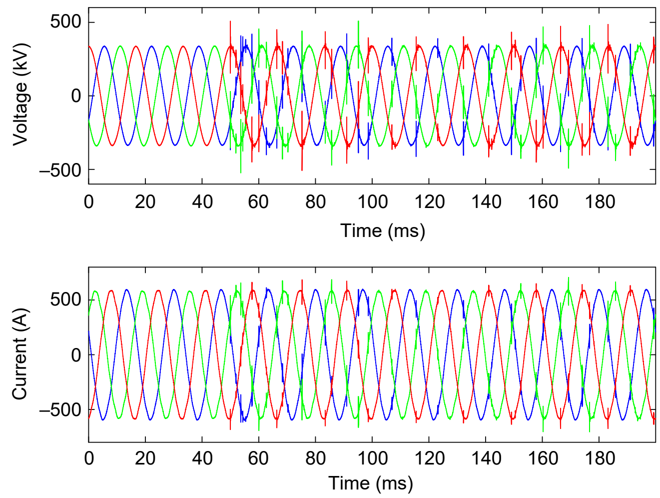


Fig. 21. High-energy discharge transient example.

It is interesting to note that the transients recorded with the megahertz sampling rate become invisible once the waveform is filtered with a linear phase second order low-pass filter and down-sampled to 10 kHz to emulate the more conventional event record, as shown in Fig. 22. In practice, this means that these high-frequency discharge transients are completely invisible to conventional protective relays.

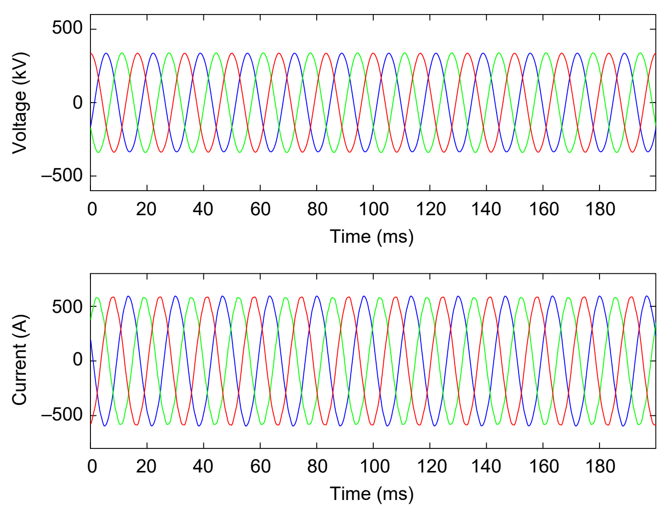


Fig. 22. Signals normally used by protective relays (Fig. 21 data down-sampled to 10 kHz).

By subtracting the low-frequency waveform in Fig. 22 from the megahertz waveform in Fig. 21, we can isolate the high-frequency discharge transients, as shown in Fig. 23.

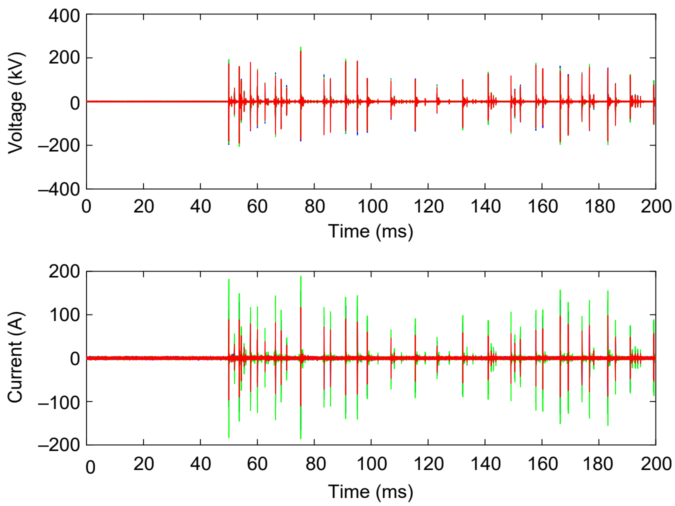


Fig. 23. High-frequency discharge transients isolated from Fig. 21.

Fig. 24 shows the signals in Fig. 23, magnified to isolate a single transient. In Fig. 24, we can identify the reflections contributed by the neighboring lines in an effort to identify the location of the transient source.

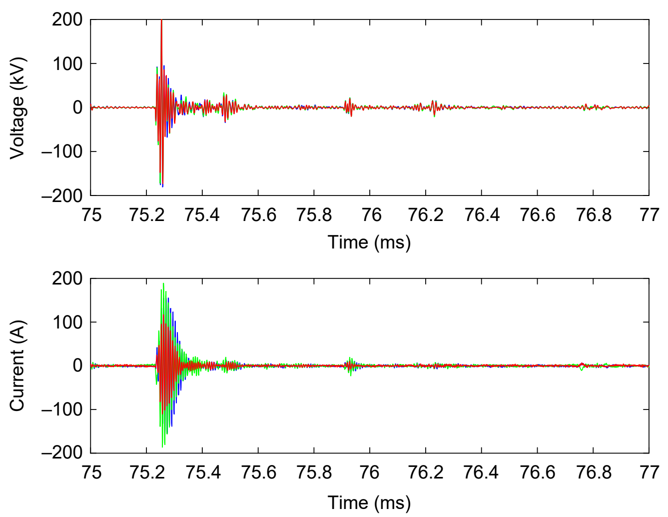


Fig. 24. Detail of Fig. 23 showing a high-frequency transient example.

With two relays strategically positioned at MID and TMD and the associated Bewley diagram shown in Fig. 25, we can determine the TW travel time and the direction of the high-energy transient source.

Fig. 25 clearly shows that the discharge events recorded at MID are real. It is also apparent that these events have enough energy to be detected after traveling for 224 km, and even 448 km, as shown by the TMD bus reflection arriving back at MID 1,580 μs after the original event. Such confirmation is very important because a similar transient could easily be coupled into the secondary wiring used to connect the relays with the instrument transformers located in the substation HV yard. The Bewley diagram in Fig. 25 also shows that the source of the transient is behind the MID relay—most likely right at the MID bus or in its immediate vicinity.

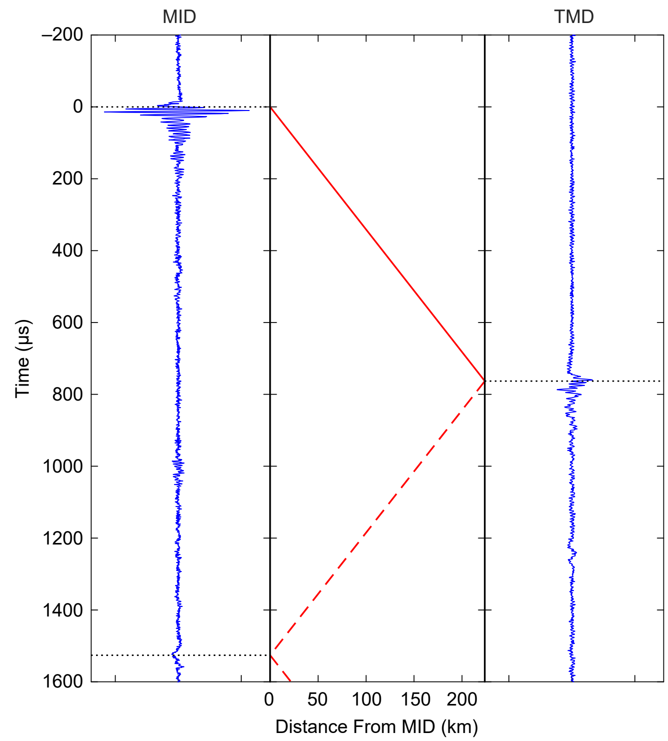


Fig. 25. A Bewley diagram shows that transients are originating behind the MID relay.

An important feature of these events is that they do not immediately lead to power system faults. They also happen during system overvoltage conditions and occur close to 60 Hz voltage peaks. Broadly speaking, recorded events fall into the partial discharge (PD) category, where one of the capacitors in a series string gets abruptly discharged by sparking over while the remaining capacitors in the string accommodate the additional voltage stress resulting from this event. The only difference is that instead of picocoulomb and nanocoulomb levels typically associated with PD, our estimate for these events reaches 50 to 200 millicoulomb levels. This estimation is based on transient modeling of the CFE network, with a high level of uncertainty caused by the lack of parasitic component data and the high frequencies involved. Nevertheless, it is supported by the transient current measurements, discharge current levels reported in [4], and the long-distance TW propagation documented in the recorded events.

Because the additional relays that would allow us to determine the exact source location are not available at this time, the best we can do is apply additional signal processing to the recordings we have.

Fig. 26 shows the result of repeatedly applying a Fourier transform and displaying it using the waterfall plot in an attempt to use TW transients to determine the local resonances excited by such transients.

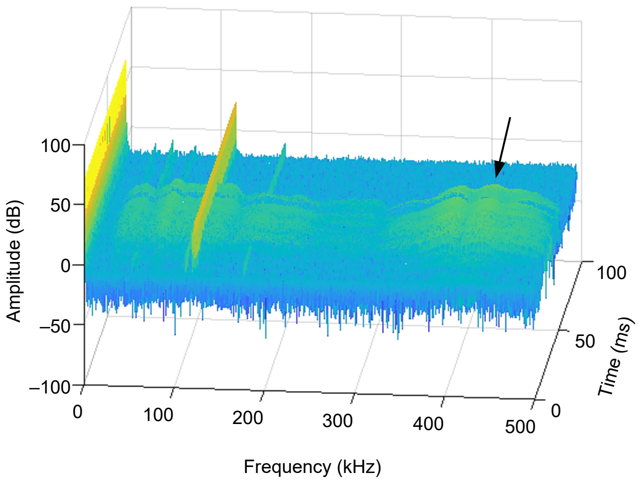


Fig. 26. Waterfall plot showing high-frequency content caused by the high-energy discharge events as a function of time.

The waterfall plot shows the PLC signal presence at 110 kHz, neighboring PLC signals with smaller magnitude, and the PLC trap high-frequency resonances excited by the transients (indicated by the arrow). Although very detailed, Fig. 26 is of little use in locating the transient discharge source.

Because each record contains multiple discharge events, with each event triggering the exact same TW reflection pattern, we can use autocorrelation to reduce the measurement noise and identify the TW reflection times. Fig. 27 shows the autocorrelation results along with the delay times associated with the known topology of the CFE system (shown in Fig. 14).

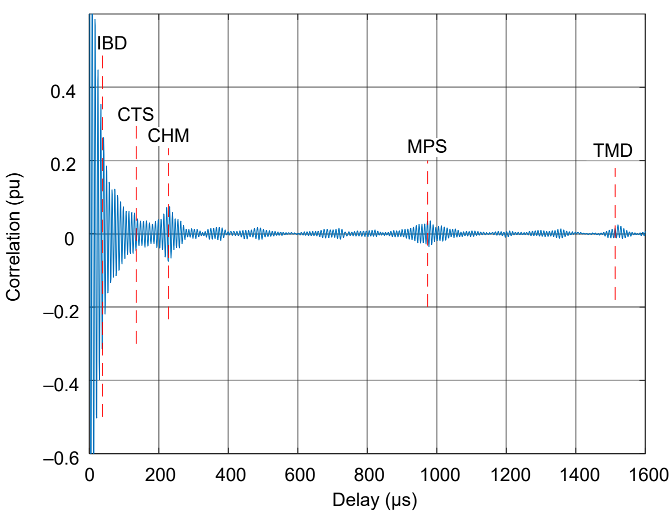


Fig. 27. Autocorrelation results with major power system reflections identified by name.

Although we cannot be completely confident, our analysis, based on the TW signature shown in Fig. 27, places the source of the reported discharge at either the MID or IBD bus. The fact that there are no shunt capacitor banks at the MID and IBD 400 kV buses and the oscillatory nature of the recorded waves point to the possibility that the transients may be injected from the lower voltage (115 kV) system. The most effective way to positively identify the location of the transient source would be to add a third relay to monitor one of the neighboring buses, such as MPS or MPD (see Fig. 14). Events originating on the TMD side of the line could be covered by adding a relay at TCL or JUI.

High-energy transients observed on the CFE 400 kV system appear to be correlated with the system voltage, are intermittent, and occur multiple times per month. Regardless, no attributable apparatus failures have occurred to date. This leads us to believe that these types of high-energy discharge events may be relatively common in HV transmission systems.

Our theory is partially confirmed with an event recorded on a 765 kV system operated by American Electric Power (AEP), with a single megahertz relay pilot in place at a substation in northwest Ohio, referred to as Substation 1 in this paper. The corresponding recording is shown in Fig. 28. Although unexplained at first, this event was soon followed by a set of three events recorded in close proximity over a 15-minute interval.

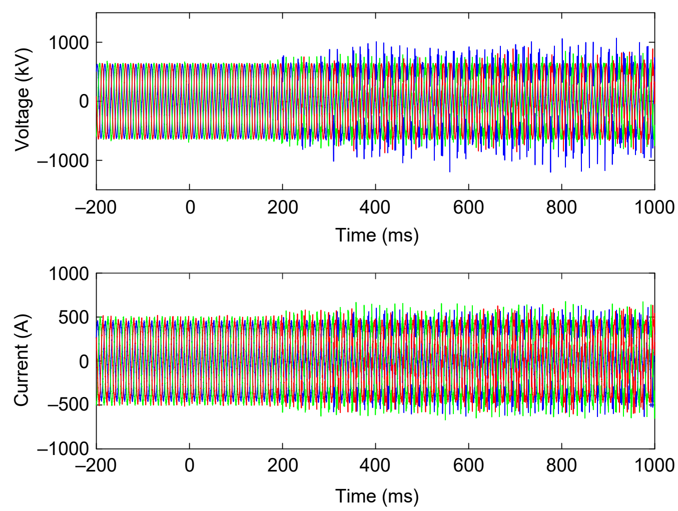


Fig. 28. High-energy discharge recorded on the 765 kV system.

The first two events in the group show the sudden appearance of very strong arcing, as shown in Fig. 29 and Fig. 30.

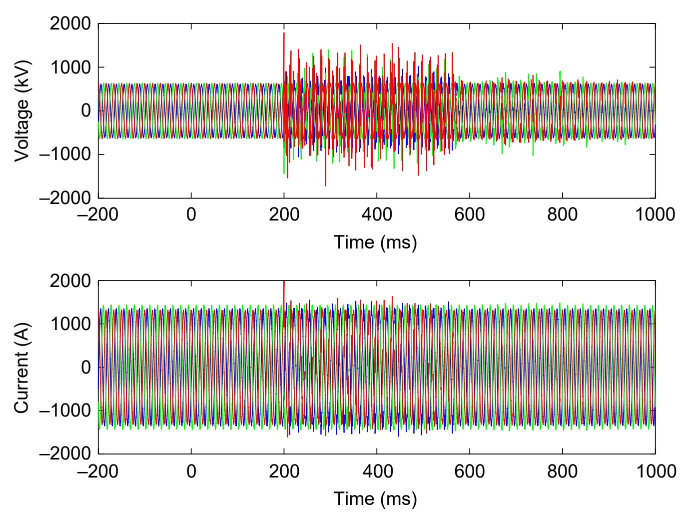


Fig. 29. First arcing event in the group.

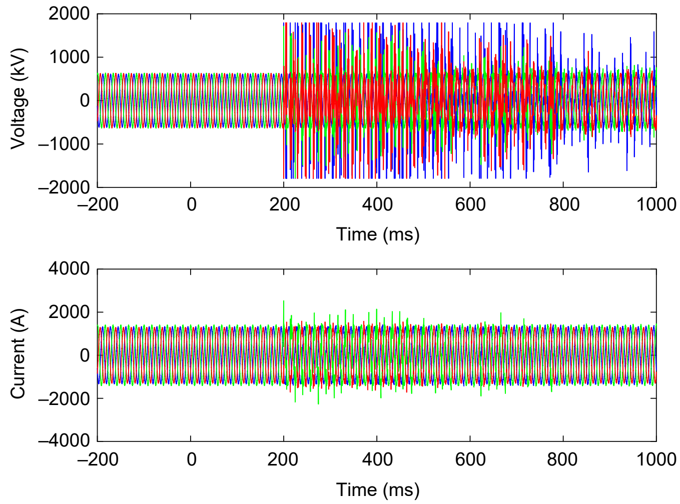


Fig. 30. Second arcing event in the group.

The voltage waveforms shown in Fig. 30 were especially troubling to AEP engineers because the relay inputs were temporarily overloaded with the last-known measurement point, apparently reaching 1,800 kV. The high-voltage reading is normal, as explained in the previous section, because the VT ratio at high frequencies is determined by the parasitic capacitance and has no relationship with the official nameplate rating of the device. However, the magnified portion of the current waveform shown in Fig. 31 is more troublesome, suggesting current transients in excess of 1 kA.

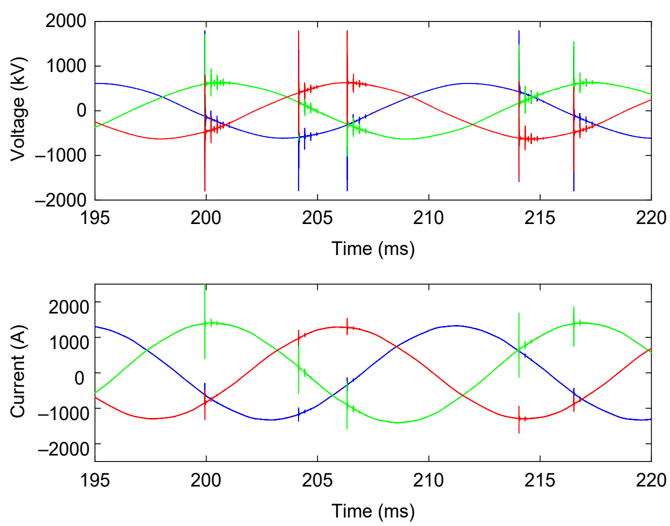


Fig. 31. Detail showing individual current transient magnitude.

The actual break in our investigation came from the third event (see Fig. 32). This event is much simpler, showing three distinct transients, with a timing pattern that is consistent with a typical breaker closing signature.

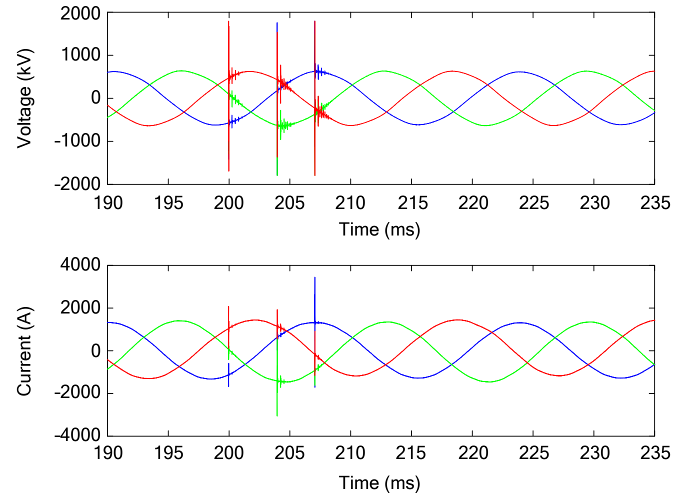


Fig. 32. Reactor breaker closing event.

In an attempt to identify this event, we contacted the AEP team and requested the SCADA alarm log for the same time period. The SCADA log is shown in Table I.

TABLE I
SEQUENCE OF EVENTS

| Time | Event | Location | SCADA Log Entry |
|---|---|---|---|
| 15:51:19 | Arcing C-Phase | Unknown | n/a |
| 15:52:36 | Arcing B-Phase | Unknown | n/a |
| 15:52:42 | n/a | Substation 1 | PLC Alarm |
| 15:52:50 | n/a | Substation 1 | PLC Alarm Clear |
| 16:05:43 | Reactor RA1 CB1 Closing | Substation 1 | CB RA1 – Reactor Closed |

The last entry in Table I clearly shows that the event in Fig. 32 captured the energizing of the shunt reactor, RA1, located at the Substation 1 bus. Knowing the exact location of this event was crucial for our effort to identify the location of the preceding two events. Being limited to a single relay location, we decided to compare the TW reflection signatures of the three events.

We started by isolating the current waveform of the active phase for each of the events and carefully aligning those waveforms in time, as shown in Fig. 33.

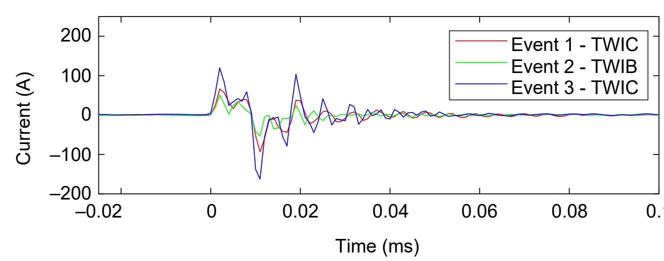


Fig. 33. Time-aligned version of the current transients recorded in the three events.

Our first surprise was the striking similarity of the current wave shapes. By adjusting the time scale, as shown in Fig. 34, we could visualize the TW signature associated with these events.

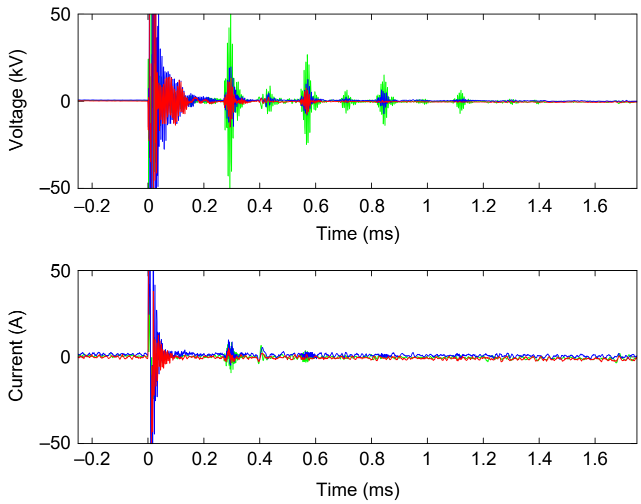


Fig. 34. TW signature for the three events on the AEP 765 kV system.

The voltage channel gain that caused clipping in Fig. 30 became helpful in this case, providing additional sensitivity and magnifying the recorded TW amplitude. To our surprise, the TW signature for the three events was an exact match, allowing us to conclude that all three events originated at Substation 1 and were closely related. Fig. 34 shows multiple reflections from the bus that is 39.7 km away, multiple reflections from the tap that is 60.6 km away, and a reflection from the line end that is 243 km away. TW reflections positively confirm that these are primary system events.

The only mystery remaining to be solved is what caused these transient events. The recorded events have the following characteristics:

- Appear suddenly
- Begin on C-phase
- Spontaneously die out
- Appear on B-phase approximately 1 minute later
- Precede breaker closing by approximately 13 minutes
- Originate at the same bus
- Are characterized by very short transients
- Are energetic enough to travel very far into the 765 kV system

Based on these characteristics, we concluded that the high-frequency transients recorded at Substation 1 were caused by the disconnect switch operation connecting the high-side of the shunt reactor breaker, CB1, to the 765 kV system. The fast high-current transient surge phenomenon is well documented in the industry [4]. It is known to cause fast transient overvoltage and is normally associated with operation of gas-insulated switchgear (GIS) disconnect switches. The AEP installation uses air-insulated disconnects. These are located between 15 and 20 meters from the GIS breakers, which may lead to somewhat lower transient frequencies. The PLC alarm reported by the SCADA system further corroborated the presence of these transients.

AEP is very interested to find the cause and actual magnitude of these high-frequency transients and understand the impact that these transients have on surrounding primary equipment, such as transformer windings. Currently, AEP is pursuing high-bandwidth instrument transformer technologies with megahertz sampling capability in order to gain more insight into power system fast transients as reported in this paper.

Although not positively confirmed at this time, we suspect that the high-frequency transients observed on the CFE system have a similar origin. Our investigation continues, but results collected to date clearly show the preventive maintenance potential of megahertz technology-based system health monitoring and the practical value of continuously monitoring the substation electromagnetic interference environment.

## VI. Evolving Fault During Single-Phase Open

Two relays with megahertz recording capabilities are monitoring the 230 kV, 28.4 km line that connects the Los Brillantes and Palo Gordo substations in Guatemala. These are owned by the Instituto Nacional de Electrificación (INDE). This line is part of the Guatemala transmission network, illustrated in Fig. 35. The relays communicate through a direct fiber-optic connection, allowing them to exchange voltage and current information in real time with measurements obtained at a one-megahertz rate. These protective relays include the incremental-quantity directional TD32 protection elements described in [5]. These elements are enabled for monitoring purposes and do not trip the line breakers. A permissive overreaching transfer trip (POTT) scheme provides primary line protection with single-phase tripping and reclosing for single-phase-to-ground faults.

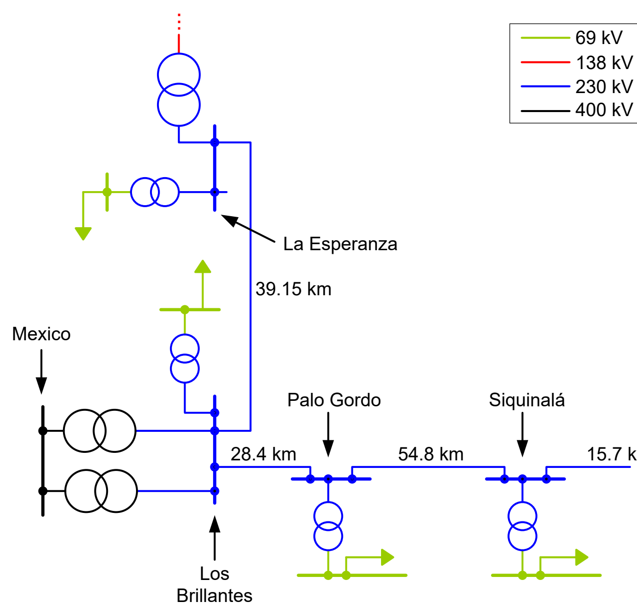


Fig. 35. Relays with a megahertz sampling rate are installed at the terminals of the 230 kV line that connects substations Los Brillantes and Palo Gordo.

On December 13, 2017, the relays recorded a C-phase to ground (CG) fault that evolved into a C-phase-to-A-phase-to-ground (CAG) fault while the C-phase was open. The oscillogram in Fig. 36 shows the voltage and current waveforms captured by the relay at Los Brillantes and the relay at Palo Gordo during the trip-reclose-trip sequence. The recording was captured by the relay located at the Los Brillantes terminal, with the Palo Gordo terminal data communicated over fiber in real time and marked on Fig. 36 as remote (VAR, IAR, etc.). Table II shows the fault durations. The CAG fault took 124.7 ms to clear at Palo Gordo because the primary protection on this line operated slowly. Fig. 36 also shows the activation of the TD32 elements in the forward direction and trip outputs at both terminals. The relays with megahertz sampling rate, which are operating in monitoring mode, activated their trip outputs (without tripping breakers) in less than 2.6 ms at the Los Brillantes and Palo Gordo terminals.

TABLE II
FAULT DURATION FOR THE CG AND CAG FAULTS

| Fault Type | Fault Duration (ms) | |
|---|---|---|
| | Los Brillantes | Palo Gordo |
| CG | 65.2 | 65.2 |
| CAG | 66.2 | 124.7 |

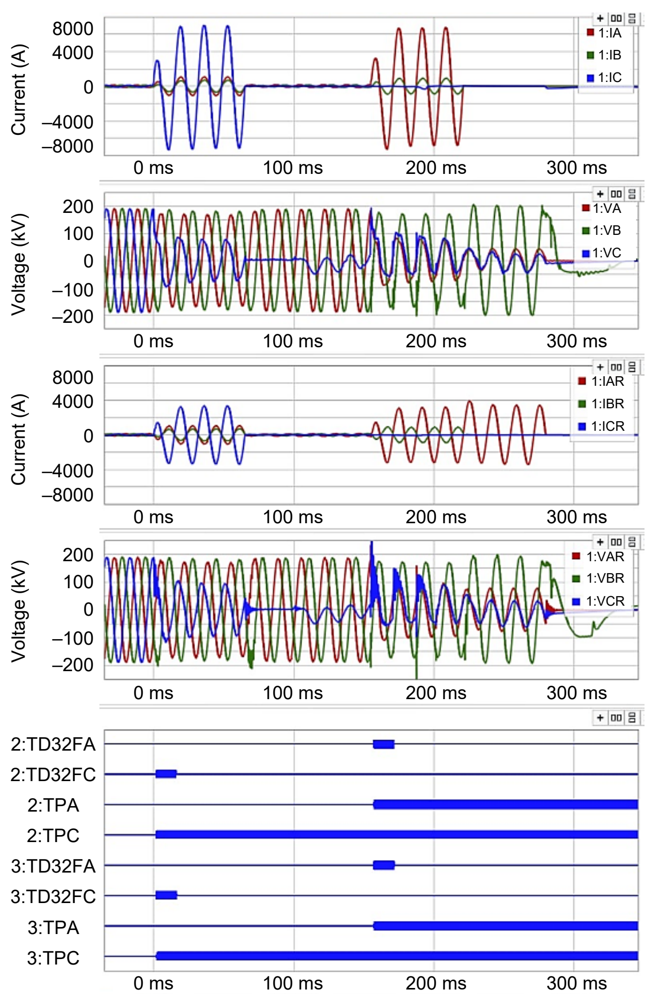


Fig. 36. TD32 element and trip assertions at Los Brillantes (2) and Palo Gordo (3) terminals for a CG fault that evolved into a CAG fault while the C-phase was open.

The voltage signals provide valuable information about the evolution of the fault. Fig. 37 shows the A-phase and C-phase voltages at Los Brillantes. The appearance of C-phase voltage during the pole-open condition indicates that the secondary arc was extinguished 108.4 ms after the CG fault initiation. At 46.1 ms later, the fault evolves into a CAG fault as the voltage difference between C-phase and A-phase collapses to zero volts, as shown in Fig. 38.

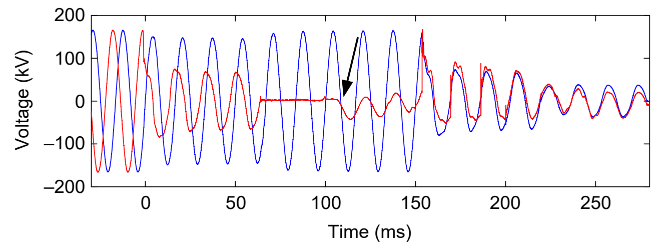


Fig. 37. Appearance of C-phase voltage during the pole-open condition indicates secondary arc extinction.

During the CAG fault condition, the arc of the fault evolves, which is indicated by changes in the C-phase-to-A-phase voltage difference, as Fig. 38 illustrates. The terminal at Los Brillantes stops feeding the CAG fault 220.6 ms after the CG fault initiation. After this instant, the Palo Gordo terminal feeds the CAG fault for another 58.6 ms. During this time, the C-phase and A-phase voltages are close to each other.

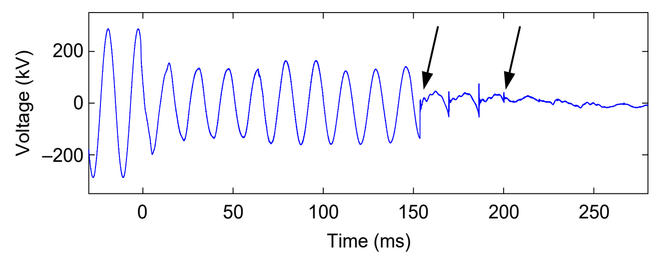


Fig. 38. C-phase-to-A-phase voltage difference close to zero volts indicates the occurrence of the CAG fault.

The full view of the event, showing voltage and current waveforms recorded simultaneously at both ends of the line, is shown in Fig. 36. High-resolution megahertz waveform recordings, which have a duration of up to 1.2 seconds, make it easy to analyze the evolution of the fault and arc conditions throughout the entire trip-reclose sequence. Voltage transients during reclosing after the fault condition are also apparent on the megahertz recording. Notice that in this event, the voltage transients did not exceed normal operating values.

## VII. CONCLUSION

Relays with megahertz sampling capabilities are providing valuable new insights into power system operation. Precise time synchronization, high-accuracy, and high-memory capacity are being combined to obtain event records with an increased level of detail.

Every new tool provides new insight and potentially a new set of worries for the system operator that was unaware that certain transients were present on the system. Widely deployed, new megahertz-capable tools are allowing us to improve condition-based monitoring and giving us the ability to proactively attack potential problems before they occur. Properly applied, we expect the new tools to bring the reliability and availability indices of our transmission network to a whole new level.

## VIII. Acknowledgment

The authors gratefully acknowledge the contributions of Bonneville Power Administration, Comisión Federal de Electricidad, American Electric Power, and Instituto Nacional de Electrificación for sharing their event records and helping to provide detailed system information necessary for analyzing these events.

## IX. References


[1] E. O. Schweitzer, III, A. Guzmán, M. V. Mynam, V. Skendzic, B. Kasztenny, and S. Marx, "Locating Faults by the Traveling Waves They Launch," proceedings of the 40th Annual Western Protective Relay Conference, Spokane, WA, October 2013.

[2] E. O. Schweitzer, III, B. Kasztenny, A. Guzmán, V. Skendzic, and M. V. Mynam, "Speed of Line Protection – Can We Break Free of Phasor Limitations?" proceedings of the 41st Annual Western Protective Relay Conference, Spokane, WA, October 2014.

[3] A. Guzmán, M. V. Mynam, V. Skendzic, J. L. Eternod, and R. M. Morales, "Directional Elements – How Fast Can They Be?" proceedings of the 44th Annual Western Protective Relay Conference, Spokane, WA, October 2017.

[4] M. Szewczyk, "Multi-Spark Modeling of Very Fast Transient Overvoltages for the Purposes of Developing HV and UHV Gas-Insulated Switchgear and of Conducting Insulation Co-ordination Studies," Bulletin of the Polish Academy of Sciences, Technical Sciences, Vol. 65, June 2017.

[5] E. O. Schweitzer, III, B. Kasztenny, and M. V. Mynam, "Performance of Time-Domain Line Protection Elements on Real-World Faults," proceedings of the 42nd Annual Western Protective Relay Conference, Spokane, WA, October 2015.


## X. Biographies

**Dr. Edmund O. Schweitzer, III** is recognized as a pioneer in digital protection and holds the grade of Fellow in the IEEE, a title bestowed on less than one percent of IEEE members. In 2002, he was elected as a member of the National Academy of Engineering. Dr. Schweitzer received the 2012 Medal in Power Engineering, the highest award given by IEEE, for his leadership in revolutionizing the performance of electrical power systems with computer-based protection and control equipment. Dr. Schweitzer is the recipient of the Regents' Distinguished Alumnus Award and Graduate Alumni Achievement Award from Washington State University and the Purdue University Outstanding Electrical and Computer Engineer Award. He has also been awarded honorary doctorates from both the Universidad Autónoma de Nuevo León, in Monterrey, Mexico, and the Universidad Autónoma de San Luis Potosí, in San Luis Potosí, Mexico, for his contributions to the development of electric power systems worldwide. He has written dozens of technical papers in the areas of digital relay design and reliability, and holds over 180 patents worldwide pertaining to electric power system protection, metering, monitoring, and control. Dr. Schweitzer received his bachelor's and master's degrees in electrical engineering from Purdue University and his doctorate from Washington State University. He served on the electrical engineering faculties of Ohio University and Washington State University, and in 1982, he founded Schweitzer Engineering Laboratories, Inc. to develop and manufacture digital protective relays and related products and services.

**Veselin Skendzic** is a principal research engineer with Schweitzer Engineering Laboratories, Inc. He earned his BS in electrical engineering from FESB, University of Split, Croatia; his masters of science from ETF, Zagreb, Croatia; and his PhD from Texas A&M University, College Station, Texas. He has more than 25 years of experience in electronic circuit design and power system protection-related problems. He is an IEEE Fellow, has written multiple technical papers, has over 20 patents, and is actively contributing to IEEE and IEC standard development. Veselin is a member of the IEEE Power Engineering Society (PES) and the IEEE Power System Relaying Committee (PSRC).

**Armando Guzmán** received his BSEE with honors from Guadalajara Autonomous University (UAG), Mexico. He received a diploma in fiber-optics engineering from Monterrey Institute of Technology and Advanced Studies (ITESM), Mexico, and his masters of science and PhD in electrical engineering and masters in computer engineering from the University of Idaho, USA. He served as regional supervisor of the Protection Department in the Western Transmission Region of the Federal Electricity Commission (the electrical utility company of Mexico) in Guadalajara, Mexico for 13 years. He lectured at UAG and the University of Idaho in power system protection and power system stability. Since 1993 he has been with Schweitzer Engineering Laboratories, Inc. in Pullman, WA, where he is a fellow research engineer. He holds numerous patents in power system protection and metering. He is a senior member of IEEE.

**Mangapathirao V. Mynam** received his MSEE from the University of Idaho in 2003 and his BE in electrical and electronics engineering from Andhra University College of Engineering, India, in 2000. He joined Schweitzer Engineering Laboratories, Inc. (SEL) in 2003 as an associate protection engineer in the engineering services division. He is presently working as a principal research engineer in SEL research and development. He was selected to participate in the U. S. National Academy of Engineering (NAE) 15th Annual U. S. Frontiers of Engineering Symposium. He is a senior member of IEEE and holds patents in the areas of power system protection, control, and fault location.

**Jean León Eternod** is the technology director for Schweitzer Engineering Laboratories, Inc. (SEL) in Mexico. Prior to joining SEL in 1998, he worked for the Comisión Federal de Electricidad (CFE) power systems studies office in protection and control corporate management. While he was at CFE from 1991 to 1998, he worked with wide-area network protection schemes; single-pole trip and reclose studies; and database validation for short circuit, load flow, and dynamic simulation, including generator and control model validation for most CFE generators. He received his BSEE from the National Autonomous University of Mexico (UNAM), where he also completed postgraduate course work in power systems. He received training in power system simulation from Power Technologies, Inc. He has authored numerous technical papers on the topics of power system protection, simulation, and wide-area protection and control applications.

**Yanfeng Gong** received his BSEE from Wuhan University, China, in 1998, his MSEE from Michigan Technological University in 2002, and his PhD in electrical engineering from Mississippi State University in 2005. He worked as a research engineer at Schweitzer Engineering Laboratories, Inc. from 2005 to 2013. He is currently working as a principal engineer/supervisor at American Electric Power (AEP) in the Advanced Transmission Studies & Technologies (ATST) department. He is a senior member of IEEE.


20190304 • TP6882-01